Universiteit
Leiden
The Netherlands

Unravelling vascular tumors : combining molecular and computational biology

IJzendoorn, D.G.P. van

Citation
IJzendoorn, D. G. P. van. (2020, January 16). *Unravelling vascular tumors : combining molecular and computational biology*. Retrieved from https://hdl.handle.net/1887/82754

Version:	Publisher's Version
License:	Licence agreement concerning inclusion of doctoral thesis in the Institutional Repository of the University of Leiden
Downloaded from:	https://hdl.handle.net/1887/82754

Note: To cite this publication please use the final published version (if applicable).

Cover Page

Universiteit Leiden

The handle http://hdl.handle.net/1887/82754 holds various files of this Leiden University dissertation.

Author: IJzendoorn, D.G.P. van
Title: Unravelling vascular tumors : combining molecular and computational biology
Issue Date: 2020-01-16

Part II

Model systems

Chapter 5

Functional analyses of a human vascular tumor FOS variant identify a novel degradation mechanism and a link to tumorigenesis

This chapter is based on the publication: **van IJzendoorn DGP**, Forghany Z, Liebelt F, Vertegaal AC, Jochemsen AG, Bovée JVMG, Szuhai K, Baker DA. Functional analyses of a human vascular tumor FOS variant identify a novel degradation mechanism and a link to tumorigenesis. *J Biol Chem.* 2017;292: 21282-21290.

5.1 Abstract

Epithelioid hemangioma is a locally aggressive vascular neoplasm, found in bones and soft tissue, whose cause is currently unknown, but may involve oncogene activation. FOS is one of the earliest viral oncogenes to be characterized, and normal cellular FOS forms part of the activator protein 1 (AP-1) transcription factor complex, which plays a pivotal role in cell growth, differentiation, and survival as well as the DNA damage response. Despite this, a causal link between aberrant FOS function and naturally occurring tumors has not yet been established. Here, we describe a thorough molecular and biochemical analysis of a mutant FOS protein we identified in these vascular tumors. The mutant protein lacks a highly conserved helix consisting of the C-terminal four amino acids of FOS, which we show is indispensable for fast, ubiquitin-independent FOS degradation via the 20S proteasome. Our work reveals that FOS stimulates endothelial sprouting and that perturbation of normal FOS degradation could account for the abnormal vessel growth typical of epithelioid hemangioma. To the best of our knowledge, this is the first functional characterization of mutant FOS proteins found in tumors.

5.2 Introduction

Epithelioid hemangioma is a neoplasm composed of cells that are phenotypically endothelial, which form vascular lumina or grow as solid sheets (figure 5.1a) (1). Until now, the molecular underpinnings of this disease have yet to be deciphered. A recent cytogenetic and karyotypic survey of the disease, by us (2) and others (3), aimed at refining diagnoses and tumor classification, unearthed a significant number of *FOS* translocations raising the possibility that disruption of FOS function could promote tumorigenesis. The immediate-early FOS proto-oncogene is activated rapidly and transiently in response to a wide spectrum of cell stimuli (4–6), including serum, growth factors, cytokines, tumor-promoting agents, and DNA damage (7). The encoded FOS protein is a component of the crucial AP-1 transcription factor complex whose normal activity is regulated by controlled proteasome degradation (8, 9), and corruption of this process can lead to cell transformation (10–12). In this study, we have investigated the role of a novel mutant FOS protein we discovered in epithelioid hemangioma. We provide evidence that sustained expression of mutant FOS, due to loss of the C terminus, might drive the formation of vascular neoplasms by perturbing matrix metalloproteinase (MMP)4 production and the Notch signaling pathway that are known to facilitate both physiological and pathological angiogenesis. Operationally, we found that the extreme C terminus of FOS renders it intrinsically susceptible to ubiquitin-independent degradation by the 20S proteasome, an essential mechanism bypassed by tumor FOS proteins. This is the first report of a module

that directly mediates ubiquitin-independent proteasomal degradation (UIPD) and emphasizes the importance of UIPD in normal as well as tumor cells. Our work establishes the first demonstrable connection between mutations of FOS and the development of a naturally occurring tumor and unveils a potential, novel approach to treating epithelioid hemangioma by targeted inhibition of FOS or proteins whose expression is activated by FOS.

5.3 Materials and Methods

5.3.1 Patient samples

Epithelioid hemangioma case L3933 was acquired from the archives of the Leiden University Medical Center (LUMC), Leiden, The Netherlands. The diagnosis of epithelioid hemangioma was established by a bone and soft tissue pathologist (J. V. M. G. B.). The study was approved by the LUMC Medical Ethical Commission under protocol B17006.

5.3.2 Cell culture, biochemistry, and molecular biology

Primary HUVECs (Lonza) were cultured in EGM2 medium (Lonza). Chondrosarcoma HT1080 and human embryonic kidney 293T cells were cultured in DMEM (Gibco) supplemented with 10% fetal bovine serum (Gibco). Transfections, lentivirus production and cell infections, Western blotting, and co-immunoprecipitations have been described previously (13). FOS stability assays were performed by incubating cells in the presence or absence of cycloheximide for a defined time course (hours). Protein levels were determined by Western blotting.

5.3.3 Plasmid and shRNA construction

Human *FOS* cDNAs fused in-frame with a *FLAG* or an *HA* epitope tag were cloned into the pLV lentiviral vector and pCS2 expression plasmid. Gene-specific shRNA-expressing lentiviruses were generated using the TRC2-pLKO lentiviral vector system.

5.3.4 Transcriptome profiling

RNA was isolated from HUVECs stably expressing FOS or FOSΔ by treatment with TRIzol (Invitrogen) column purification (Direct-zol RNA isolation kit-Zymo Research). RNA quality was verified with a Bioanalyzer (Agilent), and sequencing was performed on the Illumina HiSeq 2500 (Genome Scan). HUVEC transcript sequencing data have been deposited under GenBankTM accession no. PRJNA390521.

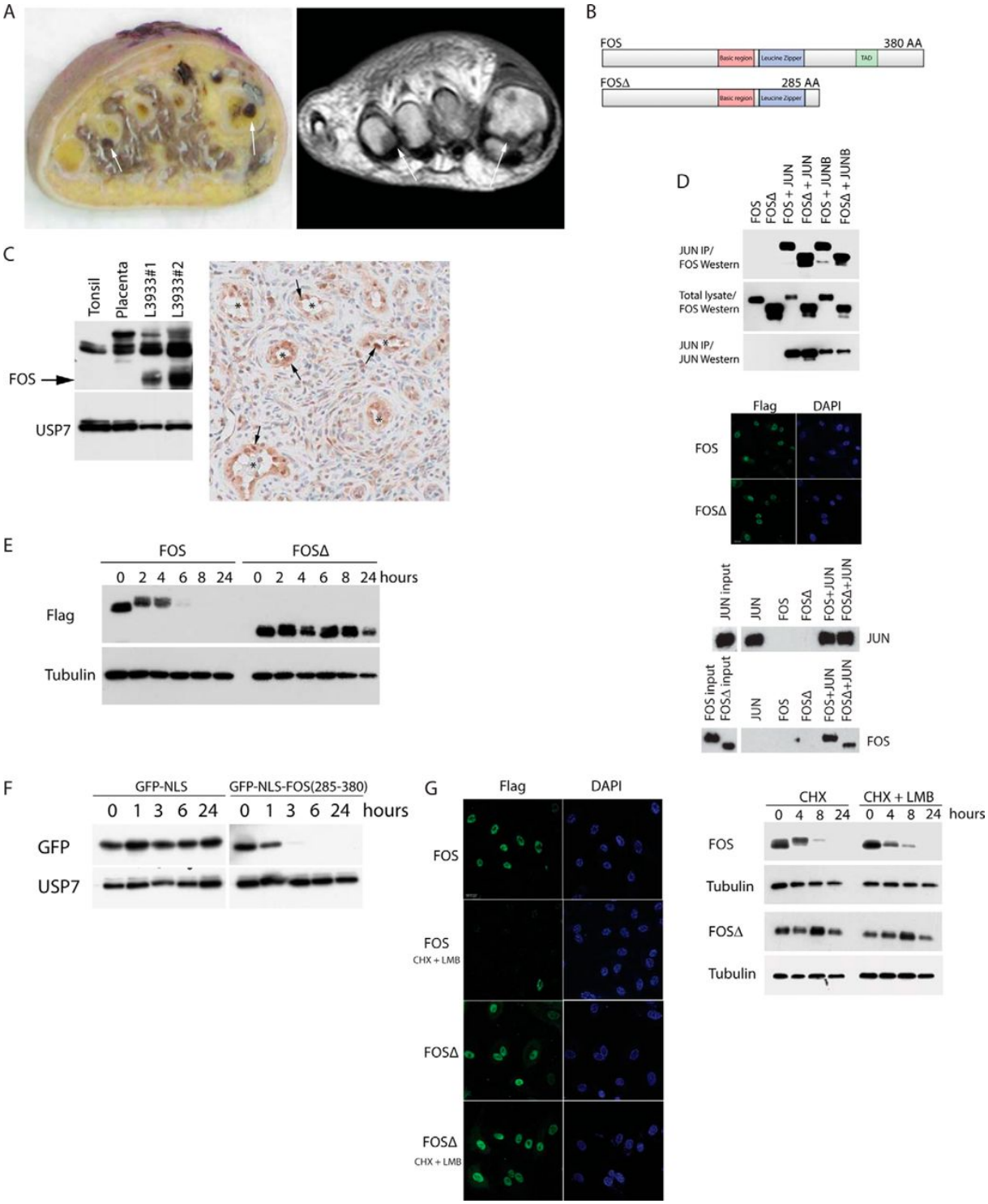

Figure 5.1: Caption on next page.

Figure 5.1: (a) Epithelioid hemangioma case L3933. Left panel, gross specimen with polyostotic localization of a hemorrhagic tumor in the 1st and 4th metatarsal bones of the foot (arrows). Right panel, corresponding T1 weighted MR image. (b) Tumor FOSΔ lacks the C-terminal 95 amino acids (including the C-terminal TAD). IP, immunoprecipitation. (c) Left panel, Western blot of endogenous FOS proteins in control tonsil and placenta cell lysates compared with epithelioid hemangioma tumor cell lysates. Mutant FOSΔ protein is highlighted with an arrow. Right panel, high FOS expression (arrows) is indicated in the endothelial cells of epithelioid hemangioma tumor blood vessels (*). (d) AP-1 heterodimers were immunopurified from cells transfected with the indicated constructs (top panel). Immunofluorescence shows both FOS and FOSΔ localize to the nucleus (middle panel). FOS (and FOSΔ), JUN heterodimers bind to consensus AP-1 DNA-binding sites (bottom panel). (e) FOS stability assay on HUVECs stably expressing FOS or FOSΔ. (f) Protein stability assay on HUVECs stably expressing either GFP or a GFP-FOS fusion (encompassing the C-terminal 95 amino acids of FOS). (g) HUVECs expressing the indicated proteins were incubated with or without leptomycin B (LMB) in the presence of cycloheximide (CHX). Left panel, immunofluorescence. Right panel, Western blots.

5.3.5 Analysis of mRNA expression

RNA isolation, first strand cDNA synthesis, and analysis of expression of transcripts by quantitative PCR were performed as described previously (14).

5.3.6 Ubiquitination assay

293T cells were transfected with the appropriate plasmids. Proteasome degradation was blocked for 8 h with 10 μm MG132 (Sigma). HIS pulldowns were performed as described previously (15).

5.3.7 HUVEC sprouting assay

96-well plates were coated with 60 μl of Matrigel/well 30 min prior to seeding HUVECs. EGM-2 medium was supplemented with 50 ng/ml recombinant human VEGF 165 (R & D Systems). Images were taken at multiple time points. Analysis of the sprouting was performed with Stacks (in-house software, Department of Molecular Cell Biology, LUMC).

5.3.8 Immunohistochemistry/Immunofluorescence

Staining was performed on 4-μm tissue sections. Paraffin was removed with xylene, and sections were rehydrated in a gradient of ethanol. Exogenous peroxidase was blocked using 0.3% H_2O_2. Microwave antigen retrieval was performed in Tris-EDTA (pH 9.0).

FOS antibody was used at a 1:400 concentration. Antibody was detected with 3,3'-diaminobenzidine, and counterstaining was performed with hematoxylin. Immunostaining was performed as described previously (15).

5.3.9 Proteasome purification and in vitro degradation assay

HT1080 cells, stably expressing GFP-PSMD12, were lysed in buffer containing 40 mm Tris (pH 7.5), 40 mm NaCl, 2 mm β-mercaptoethanol, 5 mm $MgCl_2$, 2 mm ATP, 10% glycerol, and 0.5% Nonidet P-40. Lysates were cleared by ultracentrifugation at 36,000 rpm for 45 min at 4 °C. Cleared lysates were incubated for 3 h at 4 °C with prewashed Chromotek GFP-Trap bead slurry. Beads were washed four times in wash buffer containing 40 mm Tris (pH 7.5), 40 mm NaCl, 2 mm β-mercaptoethanol, 5 mm $MgCl_2$, 2 mm ATP, and 10% glycerol. Activity of purified 26S proteasome and 20S proteasome (Enzo LifeSciences) was measured using 100 μm suc-LLVY-AMC substrate (Bachem) in a buffer containing 50 mm Tris (pH 7.5), 40 mm KCl, 5 mm $MgCl_2$, 1 mm DTT (0.5 mm ATP for the 26S proteasome) (absorbance/emission = 353/442 nm). In vitro-translated FOS proteins were prepared using the TnT-coupled reticulocyte in vitro translation system (Promega). Cell-free degradation assays were performed as described previously (16).

5.3.10 Protein-DNA interaction assays

In vitro-translated protein was made as above. 50 pmol of biotinylated double-stranded oligonucleotides harboring three contiguous AP-1 DNA-binding sites were coupled to My-One streptavidin C1 beads (Invitrogen). Reactions were incubated at 4 °C with vigorous shaking for 30 min in the presence of 1 μg of poly(dI/dC), 4 mm spermidine, 50 mm KCl, 10 mm HEPES (pH 7.6), 5 mm $MgCl_2$, 10 mm Tris (pH 8), 0.05 mm EDTA (pH 8), 0.1% Triton X-100, and 20% glycerol. Beads were successively washed three times with the aforementioned buffer. Associated proteins were eluted in Laemmli buffer, and protein-DNA interactions were determined by Western blotting.

5.3.11 ChIP

ChIP analyses were performed on confluent 10-cm tissue culture dishes of HUVECs as described previously (13).

5.3.12 Antibodies, growth factor, and drugs

Antibodies were obtained from the following sources: FLAG mouse M2 monoclonal (Sigma); anti-HA.11 mouse monoclonal (Covance); anti-FOS rabbit (Cell Signaling); anti-

HA rabbit polyclonal (Abcam); anti-FOS rabbit (Sigma); anti-FLAG rabbit (Sigma); anti-USP7 rabbit (Bethyl); anti-γ-tubulin (Sigma); anti-GFP (GeneTex); anti-His (Sigma); and anti-PSMA1 (Sigma). Drugs were used at the following concentrations: MG132 (Sigma), 10 μm; cycloheximide (Sigma), 50 μg/ml; epoxomicin (Sigma), 10 μm; leptomycin B (Sigma) 35 nm; MLN-7243 (Active Biochem), 10 μm; Batimastat (Calbiochem), 10 μm; DAPT (Tocris Bioscience), 10 μm.

5.3.13 Bioinformatics

Rosetta (RosettaCommons) was used for structure prediction of the FOS C terminus (17). Secondary structure was predicted using Psipred (version 4.01, UCL). Degree of disorder was predicted using Disopred (version 3.16, UCL).

5.4 Results and discussion

5.4.1 C-terminally truncated FOS mutant is expressed in epithelioid hemangioma

To determine whether mutations that disrupt the normal function of FOS might promote tumorigenesis, we investigated the role of a novel mutant FOS protein in epithelioid hemangioma (figure 5.1a). Figure 5.1b depicts schematically a FOS deletion mutant (hereafter termed FOSΔ) that resulted from a *FOS-MBNL1* translocation (2). The mutant transcript is predicted to encode a FOS isoform lacking the C-terminal 95 amino acids but including the bZIP domain. Western blot analysis of lysates prepared from patient tumor tissue revealed a truncated FOS protein of the expected size demonstrating that the mutant *FOS* gene is translated in vivo (figure 5.1c). Moreover, immunohistochemistry of tumor sections showed a significant enrichment of FOS in tumor blood vessel endothelial cells (figure 5.1c). In common with wild-type FOS, FOSΔ is localized to the nucleus, can heterodimerize both with JUN and JUNB, and is efficiently associated with a consensus AP-1 DNA-binding site (figure 5.1d). However, FOSΔ protein levels appear to be significantly higher than wild-type FOS protein levels in patient cells (see figure 5.1c) suggesting that the mutant protein may be aberrantly stable. To elucidate the mechanistic consequences of this deletion, we first assessed FOS protein stability in primary endothelial cells. Figure 5.1e shows that wild-type FOS, as expected, has a relatively short half-life of $\sim$1-2 h. By contrast, the deleted version of FOS is highly stable (half-life in excess of 8 h) suggesting that wild-type FOS harbors a destabilizing element in its C terminus, which is absent in the patient FOSΔ protein. In support of this view, tethering the FOS C terminus to a GFP reporter construct, led to a striking destabilization of the

GFP protein (figure 5.1f), whereas a truncated FOS C terminus did not substantially alter the stability of the GFP reporter (see figure 5.1g). This observation is consistent with previous reports relating to FOS stability (8, 18, 19). Additionally, blocking nuclear export had no effect either on rapid FOS degradation or the stability of FOSΔ indicating that FOS is degraded in the nucleus and that FOSΔ is resistant to this process (figure 5.1g). The above findings were confirmed in diploid HT1080 cell and HEK293T cells indicating that this mechanism is likely to be generic.

5.4.2 Mutant FOS is resistant to proteasomal degradation

To precisely delineate how FOS is degraded (and why FOSΔ is not), we monitored FOS protein degradation by the proteasome. Figure 5.2a shows that pharmacological inhibition of the proteasome, using either the specific inhibitor epoxomicin or MG132, markedly stabilized the wild-type FOS protein such that its half-life was comparable with that of the mutant FOSΔ protein. The half-life of FOSΔ was refractory to proteasome inhibition indicating that this deletion essentially lacks the motif(s) responsible for this degradative process (figure 5.2a). It is established that degradation by the proteasome is either ubiquitin-dependent (20) or ubiquitin-independent (21–23), and multiple different mechanisms have been reported to regulate FOS stability (24–26). In agreement with others (23, 25, 27), figure 5.2b shows that wild-type FOS can be ubiquitinated and subsequently processed by the 26S proteasome (see also figure 5.3c). We found that patient FOSΔ protein was not detectably ubiquitinated (figure 5.2b and figure 5.3c), and it fails to bind the E3 ligase, KDM2b, which has been demonstrated to stimulate FOS ubiquitination (supplementary figure S1 available online) (25). These observations could suggest that patient FOSΔ stabilization results from the absence of FOSΔ ubiquitin-dependent degradation.

However, several lines of evidence support the view that the tumor FOSΔ protein is intrinsically resistant to ubiquitin-independent proteasome degradation and that this is the principal cause of its substantially increased stability. First, pharmacological inhibition of ubiquitin-activating enzymes ablated FOS ubiquitination but had no detectable impact on FOS degradation (figure 5.2c). In the same experiment, ubiquitin-dependent degradation of an established substrate of the proteasome, MDM2, was completely abrogated (see figure 5.2c). Second, wild-type non-ubiquitinated FOS but strikingly not FOSΔ was efficiently degraded by the 20S proteasome in a cell-free in vitro system (figure 5.2d). By contrast, FOS was completely resistant to degradation by the 26S proteasome under identical conditions (figure 5.2e). Consistent with these findings, selective inhibition of the 26S proteasome, but not the 20S proteasome (through shRNA-mediated abolition of the 19S subunits PSMD2 and PSMD14), stabilized the ubiquitinated fraction of FOS but

failed to conspicuously inhibit FOS protein degradation, in sharp contrast to inhibiting both the 20S and 26S proteasomes (see figure 5.2a), indicating that degradation is principally via the 20S and not the 26S proteasome (supplementary figure S2 available online). These results show that the FOS C terminus is vital for both ubiquitin-independent and ubiquitin-dependent proteasomal degradation and that both of these processes are lost by the mutant FOSΔ protein expressed in epithelioid hemangioma. These data show that the normal process of FOS degradation is severely corrupted in the tumor FOSΔ mutant protein and substantiate previous studies (26, 28) which suggest that FOS stability is governed chiefly by ubiquitin-independent proteasome degradation.

5.4.3 Mutant FOS lacks a conserved motif essential for ubiquitin-independent degradation by the 20S proteasome

To identify the motif(s) in the C terminus of FOS, which mediates FOS degradation (and is absent in FOSΔ), we performed a thorough mutational analysis of the FOS C terminus. Figure 5.3a shows that deleting the C-terminal four amino acids was sufficient to strongly stabilize FOS and that lack of these amino acids might therefore cause the aberrant stability of the FOSΔ tumor protein. Ab initio modeling (17) of the FOS tail revealed that the C terminus is composed of an intrinsically unstructured region terminating in a helix composed of the C-terminal four amino acids (LLAL), which is conserved in all metazoans sequenced to date (figure 5.3b). Unlike FOSΔ, eliminating this helical region, either through point mutation or deletion, had no effect upon FOS ubiquitination (figure 5.3c). The same mutations did, however, efficiently block FOS degradation to the same degree as the tumor FOSΔ protein (see figure 5.3d and figure 5.3e). The integrity of the four C-terminal amino acids, but not residues immediately adjacent to this motif, is absolutely required for priming FOS labileness (figure 5.3f). Deletions or point mutations of adjacent amino acids, which include consensus phosphorylation sites for ERK and GSK, failed to augment FOS stability. Indeed, a subset of these, in agreement with others (29), served to enhance FOS instability suggesting they play a role in stabilizing but not destabilizing the FOS protein (correspondingly, chemical inhibitors of MEK or deletion of the consensus ERK-docking site had a comparable effect; data not shown). Three additional experiments further validated the importance of the C-terminal motif. One, deletion of the C-terminal four amino acids strongly attenuated the capacity of the FOS C terminus to destabilize GFP (figure 5.3g). Two, a deletion mutant lacking the intrinsically disordered region (IDR) (which is highly stable) but retaining the C-terminal four amino acids was as unstable as wild-type FOS (figure 5.3h). Three, in common with tumor FOSΔ, a mutant FOS lacking the C-terminal four amino acids, was highly resistant to 20S proteasomal degradation in a cell-free in vitro assay (figure

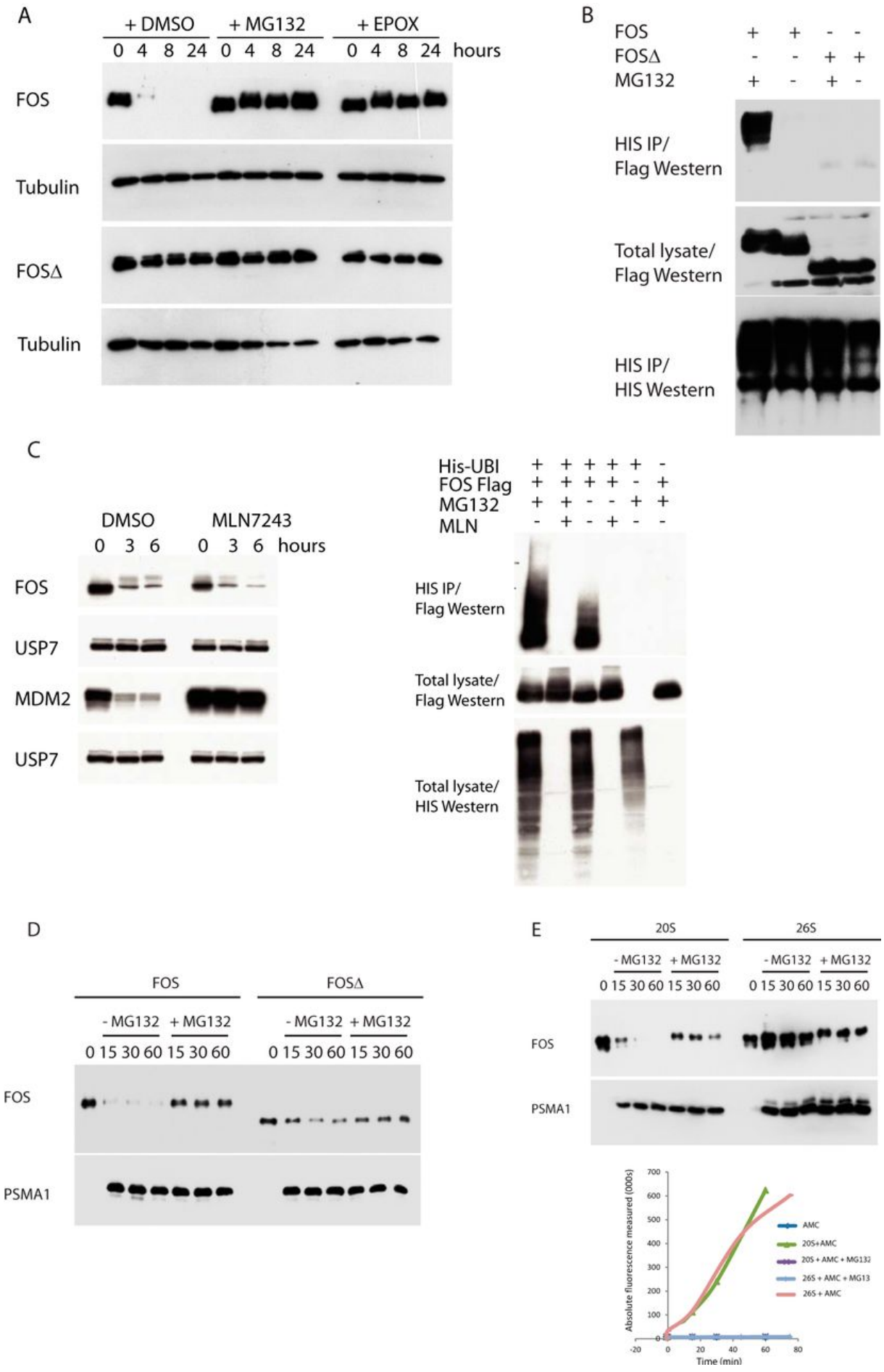

Figure 5.2: Caption on next page.

Figure 5.2: (a) FOS stability assay on HUVECs stably expressing FOS or FOSΔ. (b) Ubiquitin assay of cells transfected with the indicated constructs together with 10× HIS epitope-tagged ubiquitin. (c) Left panel, FOS stability assay on HUVECs stably expressing FOS in the presence or absence of MLN7243. Right panel, ubiquitin assay of cells transfected with the indicated constructs and cultured in the presence or absence of MG132 and MLN7243. IP, immunoprecipitation. (d) In vitro translated FOS proteins were incubated with purified 20S proteasomes for the shown time course (minutes). 20S protein levels were determined by Western blotting using an antibody directed against PSMA1. 20S proteasome activity was independently quantified using the suc-Leu-Leu-Val-Tyr-AMC peptide (as shown in e). (e) Experiment performed as in d.

5.3i). These data highlight a short helical region at the extreme C terminus of FOS as a crucial determinant of FOS stability and that perturbation of this motif leads to pronounced FOS stabilization. A block in ubiquitin-independent degradation, due to loss of the extreme C terminus, is sufficient to explain mutant FOSΔ stability. Experiments in cell-free systems indicate that this motif can orchestrate direct proteasomal degradation of FOS independently of accessory proteins. IDRs have been reported to strongly influence proteasomal degradation (30), including the IDR found in the C terminus of FOS (31). Our data show that the FOS IDR, by itself, does not stimulate FOS degradation. Rather, a highly conserved helical motif at the extreme C terminus of FOS is essential for triggering ubiquitin-independent degradation.

5.4.4 FOS potently stimulates endothelial sprouting

Vascular neoplasms result from the dysregulated growth of endothelial cells or their precursors (1) and represent a unique model for gaining insights into pathological as well as normal angiogenesis. To recapitulate the cell biological consequences of the mutant FOS stabilization observed in epithelioid hemangioma, we ectopically expressed wild-type and mutant FOS proteins in primary HUVECs and assessed their ability to sprout. Figure 5.4a shows that whereas loss of FOS abolished sprouting, sustained expression of FOS strongly promoted endothelial sprouting and the formation of stable endothelial cell networks. Similarly, expression of tumor FOSΔ or FOS lacking an intact C-terminal four amino acids strongly stimulated endothelial sprouting of HUVECs (figure 5.4b). This phenomenon was independent of marked changes in cell proliferation (figure 5.4b). Supplementary figure S3 available online shows that FOS and FOSΔ also stimulated sprouting of human lung microvascular endothelial cells. The endothelial cell networks produced by cells expressing FOS and FOSΔ were stable and persistent. In this assay, ordinarily the sprouting network is relatively short-lived and collapses after ∼24 h. By contrast, endothelial cell networks expressing elevated levels of FOS and FOSΔ were sustained for

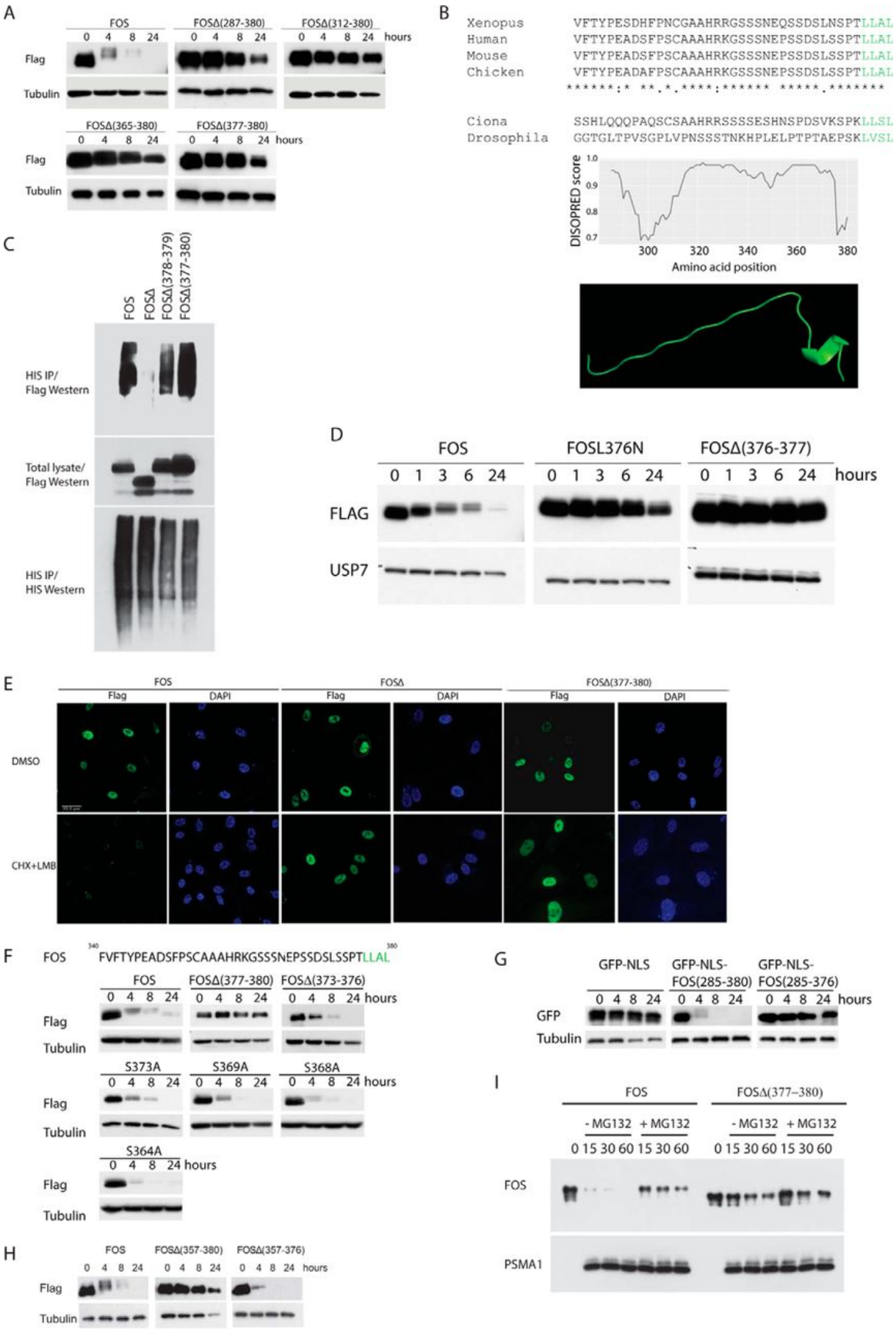

Figure 5.3: Caption on next page.

Figure 5.3: (a) FOS stability assay on HUVECs stably expressing the indicated FOS deletion mutants. (b) Ab initio modeling of the FOS C terminus. (c) Ubiquitin assay performed on cells transfected with the indicated constructs together with 10x HIS epitope-tagged ubiquitin. Cells were cultured in the presence of MG132. IP, immunoprecipitation. (d) FOS stability assay on HUVECs stably expressing the indicated FOS deletion mutants. (e) HUVECs expressing the indicated proteins were incubated with or without leptomycin B (LMB) in the presence of cycloheximide (CHX). FOS was visualized by immunofluorescence. (f) FOS stability assay on HUVECs stably expressing the indicated FOS deletion mutants. (g) Protein stability assay on HUVECs stably expressing either GFP, a GFP-FOS fusion (encompassing the C-terminal 95 amino acids of FOS), or the same fusion lacking the last four amino acids of FOS. (h) FOS stability assay on HUVECs stably expressing the indicated FOS deletion mutants. FOSΔ(357-380) lacks the C-terminal 23 amino acids (the IDR). FOSΔ(357-376) lacks the IDR but retains the C-terminal four amino acids. (i) In vitro FOS stability assay as described in figure 5.2d and figure 5.2e.

at least 2 weeks of culture (sprouting networks expressing FOSΔ were noticeably more robust than the wild-type FOS-expressing networks), which resembles the illicit vessel growth observed in human epithelioid hemangioma.

5.4.5 Mutant FOS-driven sprouting is dependent on MMPs and Notch signalling

To understand the mechanistic basis of FOS-driven sprouting, we performed global transcriptome analyses of sprouts formed by FOS or patient FOSΔ-expressing primary endothelial cells. Figure 5.4c shows a confirmatory qPCR of a selection of angiogenesis-control genes, which were up-regulated, including MMPs and components of the Notch-signaling pathway that are known to facilitate both physiological and pathological angiogenesis (14, 32–36). ChIP analyses showed that endogenous FOS bound to these promoters (supplementary figure S4 available online), and complementary ChIP studies showed that FOSΔ directly interacts with these promoters (see figure 5.4c). Our experiments uncover a previously unreported role for FOS as an activator of endothelial sprouting and show that patient FOSΔ could stimulate illicit endothelial sprouting by activating the Notch signaling pathway and increasing the production of MMPs. In this regard, it is notable that inhibitors of either MMPs or Notch signaling significantly inhibited the sprouting of FOSΔ-expressing endothelial cells (figure 5.4d). The same inhibitors had relatively little effect on cells expressing wild-type FOS under these assay conditions. This could reflect the fact that both MMP production and Notch signaling (as well as other FOS target pathways, see under "Transcriptome profiling") were significantly more augmented in cells expressing wild-type FOS compared with cells expressing FOSΔ

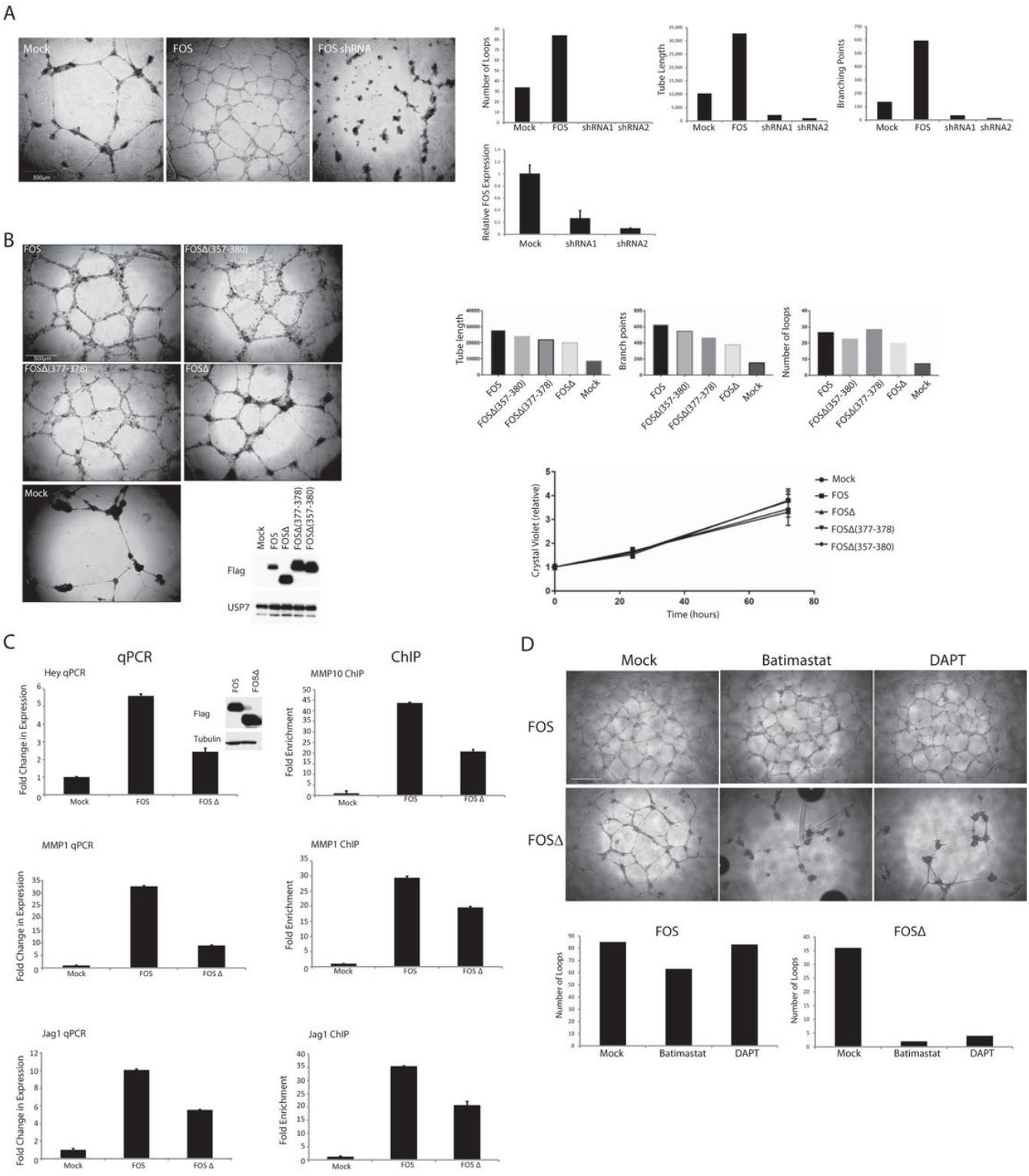

Figure 5.4: Caption on next page.

Figure 5.4: (a) HUVECs lacking endogenous FOS or ectopically expressing wild-type FOS were grown on Matrigel. A representative of several independent experiments is shown. Sprouting was quantified after 24 h using in-house computer software. Loss of *FOS* was determined by qPCR (lowermost graph). (b) Matrigel sprouting assay (see A) on HUVECs stably expressing the indicated FOS proteins. Lower graph, cell proliferation assay of the same HUVECs lines. Triplicate measurements were made at each time point. Values are means ± S.E. of the mean. (c) Left panel, expression levels of the indicated transcripts in HUVECs were determined by real-time qPCR. All values were averaged relative to TATA-binding protein (TBP), signal recognition particle receptor (SRPR), and calcium-activated neutral proteinase 1 (CAPNS1). Values were normalized against mock-treated cells. Values represent ± S.D. (n = 3). Right panel, a ChIP analysis of FOS association with the indicated promoters in HUVECs stably expressing FOS or tumor FOSΔ. Three different primer sets were used for each promoter region. A single representative is shown (all three gave similar results). Results are presented as mean fold changes in recovery (as a fraction of input) relative to the Mock infected cells. Error bars represent the standard deviation (n = 3). Relative FOS and FOSΔ protein levels were determined by Western blotting. (d) HUVECs stably expressing the indicated FOS proteins were grown on Matrigel in the presence or absence of the MMP inhibitor, batimastat (10 μM), or the γ-secretase inhibitor, DAPT (10 μM). Sprouting was quantified after 48 h.

(presumably because FOSΔ lacks the C-terminal TAD). Accordingly, a recently reported small molecule inhibitor of FOS (37), which has advanced to human Phase II clinical trials for the treatment of rheumatoid arthritis, efficiently inhibited FOS-driven endothelial sprouting (supplementary figure S5 available online).

In summary, our data have uncovered a previously unreported role for FOS in stimulating endothelial cell sprouting. We show that sustained expression of FOS, due to loss of the C terminus, could drive the formation of vascular neoplasms. By analyzing the C-terminal region of FOS, which is deleted in epithelioid hemangioma, we have discovered a highly conserved motif at the extreme C terminus of FOS that is critical for controlling its stability by rendering it intrinsically susceptible to ubiquitin-independent degradation by the 20S proteasome. Our work suggests that targeted inhibition of FOS or proteins whose expression is activated by FOS might represent a legitimate novel approach to treating these locally aggressive tumors.

Bibliography

[1] Rosenberg Ae BJ. Epithelioid haemangioma. In: Fletcher Cd BJAHPCWMF, editor. WHO Classification of Tumours of Soft Tissue and Bone. Lyon: IARC; 2013. p. 333–4.

[2] van IJzendoorn DG, de Jong D, Romagosa C, Picci P, Benassi MS, Gambarotti M, et al.

Fusion events lead to truncation of FOS in epithelioid hemangioma of bone. Genes Chromosomes Cancer. 2015;54(9):565–574. doi:10.1002/gcc.22269.

[3] Huang SC, Zhang L, Sung YS, Chen CL, Krausz T, Dickson BC, et al. Frequent FOS gene rearrangements in epithelioid hemangioma: A molecular study of 58 cases with morphologic reappraisal. American Journal of Surgical Pathology. 2015;39(10):1313–1321. doi:10.1097/PAS.0000000000000469.

[4] Jochum W, Passegue E, Wagner EF. AP-1 in mouse development and tumorigenesis. Oncogene. 2001;20(19):2401–2412. doi:10.1038/sj.onc.1204389.

[5] Johnson RS, Spiegelman BM, Papaioannou V. Pleiotropic effects of a null mutation in the c-fos proto-oncogene. Cell. 1992;71(4):577–86.

[6] Shaulian E, Karin M. AP-1 as a regulator of cell life and death. Nat Cell Biol. 2002;4(5):E131–6. doi:10.1038/ncb0502-e131.

[7] Haas S, Kaina B. c-Fos is involved in the cellular defence against the genotoxic effect of UV radiation. Carcinogenesis. 1995;16(5):985–91.

[8] Wilson T, Treisman R. Fos C-terminal mutations block down-regulation of c-fos transcription following serum stimulation. The EMBO journal. 1988;7(13):4193–202.

[9] Gomard T, Jariel-Encontre I, Basbous J, Bossis G, Mocquet-Torcy G, Piechaczyk M. Fos family protein degradation by the proteasome. Biochemical Society Transactions. 2008;36(5):858–863. doi:10.1042/BST0360858.

[10] Van Beveren C, van Straaten F, Curran T, Müller R, Verma IM. Analysis of FBJ-MuSV provirus and c-fos (mouse) gene reveals that viral and cellular fos gene products have different carboxy termini. Cell. 1983;32(4):1241–55.

[11] Eferl R, Wagner EF. AP-1: A double-edged sword in tumorigenesis. Nature Reviews Cancer. 2003;3(11):859–868. doi:10.1038/nrc1209.

[12] Monje P, Marinissen MJ, Gutkind JS. Phosphorylation of the carboxyl-terminal transactivation domain of c-Fos by extracellular signal-regulated kinase mediates the transcriptional activation of AP-1 and cellular transformation induced by platelet-derived growth factor. Molecular and cellular biology. 2003;23(19):7030–43. doi:10.1128/MCB.23.19.7030-7043.2003.

[13] Roukens MG, Alloul-Ramdhani M, Baan B, Kobayashi K, Peterson-Maduro J, Van Dam H, et al. Control of endothelial sprouting by a Tel-CtBP complex. Nature Cell Biology. 2010;12(10):933–942. doi:10.1038/ncb2096.

[14] Adams RH, Alitalo K. Molecular regulation of angiogenesis and lymphangiogenesis. Nature Reviews Molecular Cell Biology. 2007;8(6):464–478. doi:10.1038/nrm2183.

[15] Roukens MG, Alloul-Ramdhani M, Moghadasi S, Op den Brouw M, Baker DA. Down-regulation of vertebrate Tel (ETV6) and Drosophila Yan is facilitated by an evolutionarily conserved mechanism of F-box-mediated ubiquitination. Mol Cell Biol. 2008;28(13):4394–4406. doi:10.1128/MCB.01914-07.

[16] Asher G, Tsvetkov P, Kahana C, Shaul Y. A mechanism of ubiquitin-independent proteasomal degradation of the tumor suppressors p53 and p73. Genes & development. 2005;19(3):316–21. doi:10.1101/gad.319905.

[17] Baker D. Centenary Award and Sir Frederick Gowland Hopkins Memorial Lecture. Protein folding, structure prediction and design. Biochemical Society transactions. 2014;42(2):225–9. doi:10.1042/BST20130055.

[18] Ferrara P, Andermarcher E, Bossis G, Acquaviva C, Brockly F, Jariel-Encontre I, et al. The structural determinants responsible for c-Fos protein proteasomal degradation differ according to the conditions of expression. Oncogene. 2003;22(10):1461–1474. doi:10.1038/sj.onc.1206266.

[19] Acquaviva C, Brockly F, Ferrara P, Bossis G, Salvat C, Jariel-Encontre I, et al. Identification of a C-terminal tripeptide motif involved in the control of rapid proteasomal degradation of c-Fos proto-oncoprotein during the G(0)-to-S phase transition. Oncogene. 2001;20(51):7563–7572. doi:10.1038/sj.onc.1204880.

[20] Collins GA, Goldberg AL. The Logic of the 26S Proteasome. Cell. 2017;169(5):792–806. doi:10.1016/J.CELL.2017.04.023.

[21] Erales J, Coffino P. Ubiquitin-independent proteasomal degradation. Biochimica et Biophysica Acta (BBA) - Molecular Cell Research. 2014;1843(1):216–221. doi:10.1016/J.BBAMCR.2013.05.008.

[22] Jariel-Encontre I, Bossis G, Piechaczyk M. Ubiquitin-independent degradation of proteins by the proteasome. Biochim Biophys Acta. 2008;1786(2):153–177. doi:10.1016/j.bbcan.2008.05.004.

[23] Ben-Nissan G, Sharon M. Regulating the 20S proteasome ubiquitin-independent degradation pathway. Biomolecules. 2014;4(3):862–884. doi:10.3390/biom4030862.

[24] Stancovski I, Gonen H, Orian A, Schwartz AL, Ciechanover A. Degradation of the proto-oncogene product c-Fos by the ubiquitin proteolytic system in vivo and in vitro: identification and characterization of the conjugating enzymes. Molecular and cellular biology. 1995;15(12):7106–16. doi:10.1128/MCB.15.12.7106.

[25] Han XR, Zha Z, Yuan HX, Feng X, Xia YK, Lei QY, et al. KDM2B/FBXL10 targets c-Fos for ubiquitylation and degradation in response to mitogenic stimulation. Oncogene. 2016;35(32):4179–4190. doi:10.1038/onc.2015.482.

[26] Adler J, Reuven N, Kahana C, Shaul Y. c-Fos Proteasomal Degradation Is Activated by a Default Mechanism, and Its Regulation by NAD(P)H:Quinone Oxidoreductase 1 Determines c-Fos Serum Response Kinetics. Molecular and Cellular Biology. 2010;30(15):3767–3778. doi:10.1128/MCB.00899-09.

[27] Basbous J, Chalbos D, Hipskind R, Jariel-Encontre I, Piechaczyk M. Ubiquitin-independent proteasomal degradation of Fra-1 is antagonized by Erk1/2 pathway-mediated phosphorylation of a unique C-terminal destabilizer. Mol Cell Biol. 2007;27(11):3936–3950. doi:10.1128/MCB.01776-06.

[28] Sasaki T, Kojima H, Kishimoto R, Ikeda A, Kunimoto H, Nakajima K. Spatiotemporal Regulation of c-Fos by ERK5 and the E3 Ubiquitin Ligase UBR1, and Its Biological Role. Molecular Cell. 2006;24(1):63–75. doi:10.1016/j.molcel.2006.08.005.

[29] Okazaki K, Sagata N. The Mos/MAP kinase pathway stabilizes c-Fos by phosphorylation and augments its transforming activity in NIH 3T3 cells. The EMBO journal. 1995;14(20):5048–59.

[30] Prakash S, Tian L, Ratliff KS, Lehotzky RE, Matouschek A. An unstructured initiation site is required for efficient proteasome-mediated degradation. Nature Structural & Molecular Biology. 2004;11(9):830–837. doi:10.1038/nsmb814.

[31] Campbell KM, Terrell AR, Laybourn PJ, Lumb KJ. Intrinsic structural disorder of the C-terminal activation domain from the bZIP transcription factor Fos. Biochemistry. 2000;39(10):2708–2713. doi:10.1021/bi9923555.

[32] Heo SH, Choi YJ, Ryoo HM, Cho JY. Expression profiling of ETS and MMP factors in VEGF-activated endothelial cells: Role of MMP-10 in VEGF-induced angiogenesis. Journal of Cellular Physiology. 2010;224(3):734–742. doi:10.1002/jcp.22175.

[33] Lee S, Jilani SM, Nikolova GV, Carpizo D, Iruela-Arispe ML. Processing of VEGF-A by matrix metalloproteinases regulates bioavailability and vascular patterning in tumors. The Journal of Cell Biology. 2005;169(4):681–691. doi:10.1083/jcb.200409115.

[34] Kopan R, Ilagan MXG. The Canonical Notch Signaling Pathway: Unfolding the Activation Mechanism. Cell. 2009;137(2):216–233. doi:10.1016/j.cell.2009.03.045.

[35] Herbert SP, Stainier DYR. Molecular control of endothelial cell behaviour during blood vessel morphogenesis. Nature Reviews Molecular Cell Biology. 2011;12(9):551–564. doi:10.1038/nrm3176.

[36] Juncker-Jensen A, Deryugina EI, Rimann I, Zajac E, Kupriyanova TA, Engelholm LH, et al. Tumor MMP-1 Activates Endothelial PAR1 to Facilitate Vascular Intravasation and Metastatic Dissemination. Cancer Research. 2013;73(14):4196–4211. doi:10.1158/0008-5472.CAN-12-4495.

[37] Ye N, Ding Y, Wild C, Shen Q, Zhou J. Small molecule inhibitors targeting activator protein 1 (AP-1). Journal of Medicinal Chemistry. 2014;57(16):6930–6948. doi:10.1021/jm5004733.